Langmuir
Article
pubs.acs.org/Langmuir

Adsorption Behavior of Asymmetric Pd Pincer Complexes on a Cu(111) Surface

Shih-Hsin Chang,[†,§] Alessandro Scarfato,[†,‡] Christian Kleeberg,[⊥] Martin Bröring,[⊥] Germar Hoffmann,*[,†] and Roland Wiesendanger[†]

[†]*Institute of Applied Physics and Microstructure Research Center Hamburg, University of Hamburg, Germany,* [‡]*Dipartimento di Fisica "E.R. Caianiello", Università degli Studi di Salerno, Italy, and* [⊥]*Fachbereich Chemie, Philipps-Universität Marburg, Germany.* [§]*Present address: Research Center for Applied Sciences, Academia Sinica, Taipei, Taiwan*

Received February 19, 2010. Revised Manuscript Received April 3, 2010

We address the adsorption of asymmetric Pd pincer complexes on a Cu(111) surface by scanning tunneling microscopy. The structural asymmetry is manifested in the observation of two chiral enantiomers. To enable an unambiguous identification of individual constituents, three closely related complexes with small modifications are investigated in parallel. Thereby, methyl substituents determine attractive molecule−molecule interaction. Depending on their distribution, dimerization and tetramerization can be observed.

Introduction

Palladium-containing organometallics and, in particular, pincer type complexes of this class of inorganics are important functional molecules for organic synthesis and catalysis.[1] Palladium pincer complexes have recently been introduced in several topical fields like C−C coupling catalysis, C−H bond activation, sensoric materials, or biohybrids, to name a few.[2] Whereas cobalt and nickel containing pincer compounds are well-established catalysts and have even found entry in technical processes, the potential of palladium pincers to activate rather inert bonds[3] and to efficiently induce stereoselective processes[4] was only recently realized. The design of asymmetric Pd pincer complexes adds further possibilities for the tailoring of reaction processes.[5] Moreover, some of the studied asymmetric Pd pincer complexes show a unique porous bulk structure.[6] This opens additional opportunities for the construction of heterogeneous catalysts by the molecules-to-materials approach, or by organizing catalytically active molecules on surfaces via anchoring side groups.[7] However, few is known so far about the formation process and the local properties, and local studies on palladium pincer complexes on surfaces have not yet been reported.

Here, we demonstrate the preparation and adsorption of three asymmetric Pd pincer complexes on a metallic substrate. Scanning tunneling microscopy (STM) is used for the investigation of the adsorption behavior, first to identify single complexes, then to observe the beginning of the aggregation process. Model molecular electronic structure calculations for asymmetric Pd pincer complexes in the vicinity of a metallic substrate are currently not available. Because of the lack of any rotational and mirror symmetry the computational unit cell will be large and calculations rather complex. Moreover, the adsorption site is not avialable as input for the modeling. Instead, we chose a systematic approach via ligand modification for the analysis of the acquired STM images.

A pincer complex consists of a meridional tridentate ligand (pincer ligand) hosting a metal atom which in this case is a palladium(II) ion. For illustration, Figure 1a presents a space-filling model for one of the used substances (**2**), with the structure deduced from its bulk phase. The palladium(II) ion is coordinated in distorted square-planar geometry by three N donor atoms and by a C(sp^3) atom from a C−H activated *tert*-butyl substituent. The remaining moieties of this pincer ligand (thiazole, pyridine and benzene ring) are approximately in plane with the PdN_3C coordination center, whereas one of the methyl substituents of the *tert*-butyl group protudes into the third dimension. For the present study, small modifications are introduced as depicted in the structural formulas of the employed complexes (4-MeBtPI*)Pd (**1**), (4-tBuTPI*)Pd (**2**), and (4-tBu-6-MeBtPI*)Pd (**3**); see Figure 1b. The synthesis of these complexes is described elsewhere.[6,8]

Experimental Section

STM. All experiments were performed in an ultrahigh vacuum environment. Cu(111) surfaces were cleaned by repeated cycles of Ar^+ ion etching and annealing to ∼900 K. Surface cleanness was verified before deposition of molecules by STM. Molecules were sublimed from molecular powders in homemade Knudsen cells after thorough degassing (up to 12 h) with the evaporation rate monitored by a quartz-crystal microbalance. During deposition, substrate surfaces were precooled to ∼200 K and afterward immediately transferred to the STM. The STM was operated at 25−30 K during the measurements.[9] As STM probes electrochemically etched tungsten tips were used. Bias voltages refer to the sample potential with respect to the tip; i.e., positive values

*To whom correspondence should be addressed. E-mail: ghoffman@physnet.uni-hamburg.de Phone: +49-40-42838-6201. Fax: +49-40-42838-2944.

(1) Dupont, J.; Consorti, C.; Spencer, J. *Chem. Rev.* **2005**, *105*, 2527–2571.
(2) Albrecht, M.; van Koten, G. *Angew. Chem., Int. Ed.* **2001**, *40*, 3750–3781.
(3) Bröring, M.; Kleeberg, C. *Chem. Commun.* **2008**, 2777–2778.
(4) Langlotz, B.; Wadepohl, H.; Gade, L. *Angew. Chem., Int. Ed.* **2008**, *47*, 4670–4674.
(5) Bröring, M.; Kleeberg, C.; Köhler, S. *Inorg. Chem.* **2008**, *47*, 6404–6412.
(6) Kleeberg, C.; Bröring, M. *Polyhedron* **2010**, *29*, 507–513.
(7) Kleij, A. W.; Gossage, R. A.; Jastrzebski, J. T. B. H.; Boersma, J.; van Koten, G. *Angew. Chem., Int. Ed.* **2000**, *39*, 176–178.
(8) Manuscript on the syntheses of complexes **1** and **3** in preparation.
(9) Kuck, S.; Wienhausen, J.; Hoffmann, G.; Wiesendanger, R. *Rev. Sci. Instrum.* **2008**, *79*, 083903.

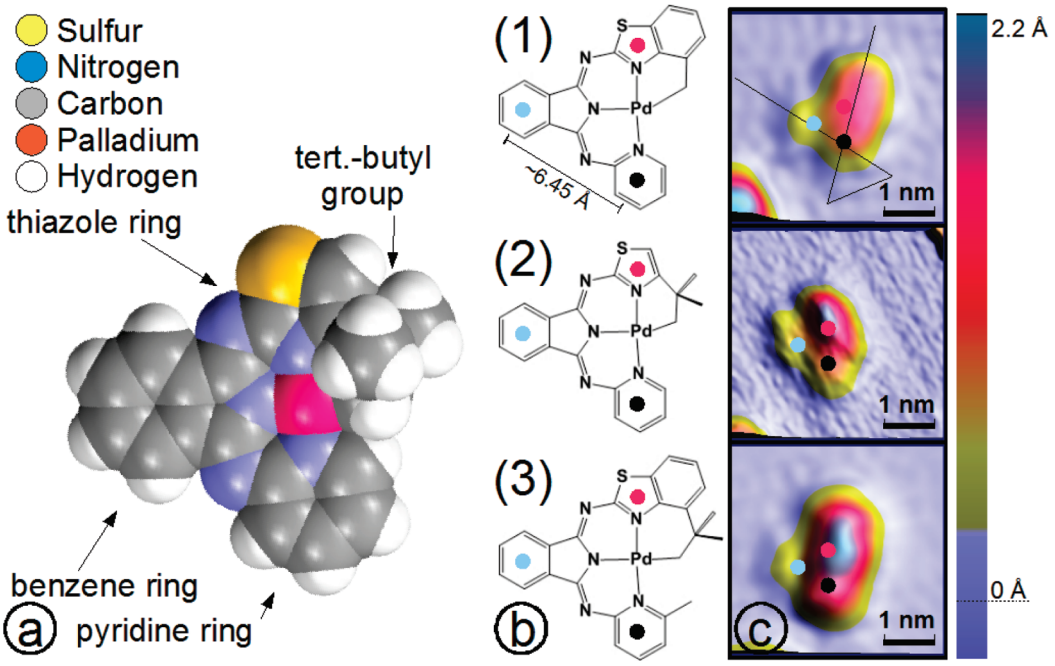

Figure 1. (a) Three-dimensional ball model of complex **2**. (b) Chemical structures of (4-MeBtPI*)Pd (**1**), (4-tBuTPI*)Pd (**2**), and (4-tBu-6-MeBtPI*)Pd (**3**) with markers for the benzene, the thiazole, and the pyridine rings as used throughout the images of the article. (c) STM images of complexes **1**−**3** after adsorption on a clean Cu(111) surface with superimposed markers at the corresponding scale (the indicated color bar equally holds for images 3c, 3d, and 3e). The lines indicate the positions of the line profiles in Figure 2 crossing the maxima of **1**. (Scanning parameters in part c): (1) −0.5 V, 150 pA, 4 × 4 nm^2; (2) −0.4 V, 143 pA, 4 × 4 nm^2; (3) −0.5 V, 150 pA, 4 × 4 nm^2.).

indicate tunneling into unoccupied sample states. Images shown in this paper represent raw data after line flattening.[10]

Results

Figure 1c shows STM images of the isolated complexes after adsorption on Cu(111) at $U \simeq -0.5$ eV. No significant bias dependence (not shown) is observed indicating a strong hybridization of molecular and substrate states. The images are aligned corresponding to the chemical structures.[11] For orientation, we marked three well-defined positions in the plane of complex **1**, the center of one benzene ring, the thiazole, and of the pyridine ring. These positions are projected at the corresponding scales on top of the other structures as well as on the STM images. Because of the experimental approach via contacting the surrounding electron cloud, molecules appear respectively larger than in their atomic structures. All species are asymmetric in their STM images with one protrusion and two pronounced shoulders evolving at different heights as plotted color encoded. These features mainly originate from the benzene and pyridine rings as well as from the *tert*-butyl group. For complexes **2** and **3** the *tert*-butyl moiety is the dominating feature due to its extension below and above the molecular plane. This corresponds to previous STM observations on *tert*-butyl substituted molecules.[12] The weakest feature in the STM images can be attributed to the benzene ring of the central isoindoline moiety, whereas the remaining shoulder originates from the electron cloud above the pyridine ring.

Figure 2 presents line sections from mixed samples, i.e., (a) with complexes **1** and **2** present at the same time on the identical Cu(111) surface and (b) for complexes **1** and **3** adsorbed on Cu(111). Molecules selected are oriented in parallel to each other. These precautions avoid additional complications due to the unknown tip geometry and electronic state of the tip and enable a qualitative comparison. Line sections start on the bare Cu(111) surface and cross the three characteristic topographical features along two axes as indicated in Figure 1c. We find, identical molecular subunits are imaged at approximately the same topographical heights, confirming our previously introduced assignment of topographical features. The contribution of a high density of electron states above the methyl group in complex **3** and the Pd coordinated *tert*-butyl group in complexes **2** and **3** is significant. In the latter case, steric repulsion causes an upward orientation of one of the methyl extensions (see also Figure 1a) and shifts the cloud of the respective electron states above the molecular plane.

A direct consequence of the chemical structures is the lack of any in-plane rotational symmetry. Therefore, surface supported chirality, also called prochirality, is observed for isolated molecules.[13] Left- and right-handed enantiomers in six orientations—due to the 6-fold symmetry of the Cu(111) surface—are identified; Figure 3a illustrates the positions of all 12 adsorption geometries relative to the ⟨1−10⟩ axis of the substrate for **2**. Figure 3b shows a representative larger image with the adsorption geometries indicated. Whereas most molecules stay isolated, few larger units can be observed. Molecules retain their preferable adsorption geometry within dimers. Whereas in tetramers (see for example Figure 3c),

(10) Horcas, I.; Fernandez, R.; Gomez-Rodriguez, J.; Colchero, J.; Gomez-Herrero, J.; Baro, A. M. *Rev. Sci. Instrum.* **2007**, *78*, 013705.

(11) Note: Each protusion in the STM images can be unambigously attributed to a specific molecular subunit. Due to the preparation of bimolecular systems, the parallel alignment of the benzene-pyridine axis is granted within the experimental series. Whereas an assignment of topographical features to exact positions in the chemical structure is not given (Δx, Δy = 0.2 nm, $\Delta\theta$ = 10°). As isolated molecules and clusters of homochiral molecules are predominant, the systematic uncertainty has no impact on the analysis.

(12) (a) Jung, T. A.; Schlittler, R. R.; Gimzewski, J. K. *Nature* **1997**, *386*, 696–698. (b) Hoffmann, G.; Libioulle, L.; Berndt, R. *Phys. Rev. B* **2002**, *65*, 212107. (c) Deng, Z. T.; Guo, H. M.; Guo, W.; Gao, L.; Cheng, Z. H.; Shi, D. X.; Gao, H.-J. *J. Phys. Chem. C* **2009**, *113*, 11223–11227.

(13) (a) Böhringer, M.; Schneider, W.-D.; Berndt, R. *Angew. Chem., Int. Ed.* **2000**, *39*, 792–795. (b) Ernst, K.-H. *Top. Curr. Chem.* **2006**, *265*, 209–252. (c) Kuck, S.; Hoffmann, G.; Bröring, M.; Fechtel, M.; Funk, M.; Wiesendanger, R. *J. Am. Chem. Soc.* **2008**, *130*, 14072–14073. (d) Bombis, C.; Weigelt, S.; Knudsen, M. M.; Nørgaard, M.; Busse, C.; Lægsgaard, E.; Besenbacher, F.; Gothelf, K. V.; Linderoth, T. R. *ACS Nano* **2010**, *4*, 297–311.

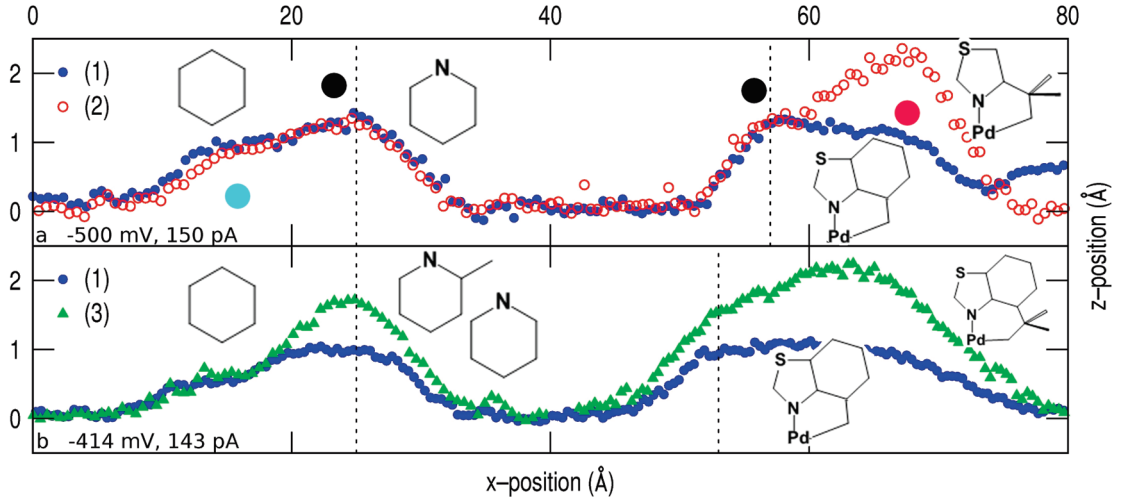

Figure 2. Line sections through STM images of complexes **1**−**3** along the phenyl−pyridine axis and the pyridine−thiazole axis. Within each graph, the probing tip is identical and selected molecules are aligned parallel to each other; this avoids complications due to the unknown tip shape and electronic tip state. For orientation, dotted lines indicate the same position above the molecules within individual line sections.

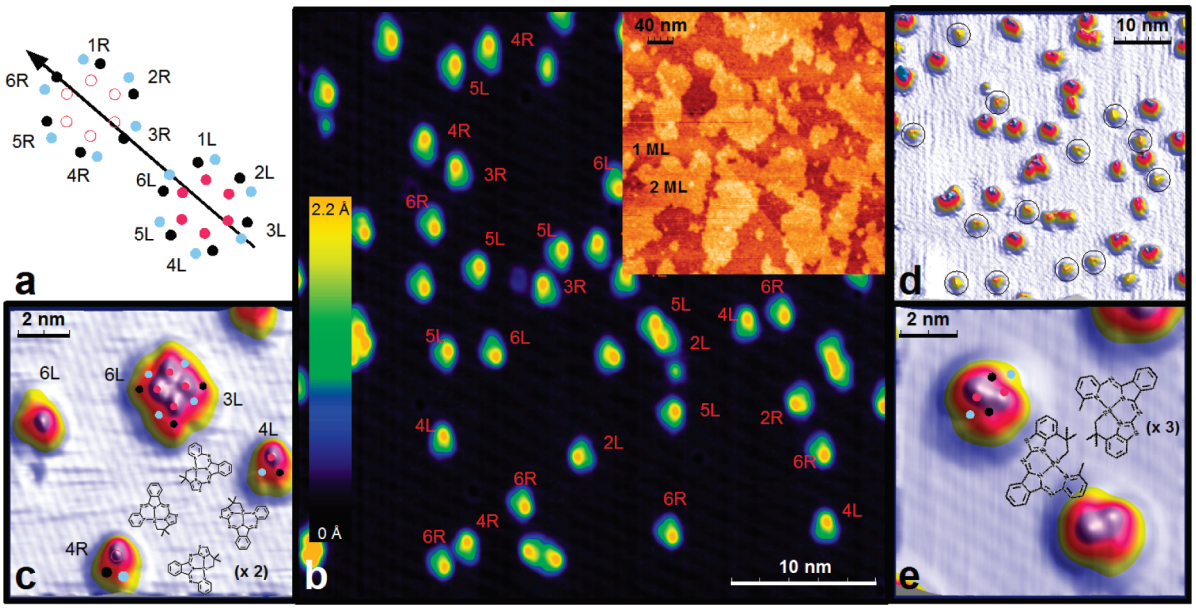

Figure 3. (a) Arrangements of complex **2** relative to the <1−10> substrate axis for left- (●) and right (○) -handed molecules. The colors correspond to chemical groups as introduced in Figure 1. Because of the 6-fold symmetry of the surface, six (1−6) orientations are found for each enantiomer (*L*, *R*). (b) STM image of a larger surface area with the adsorption geometry of complex **2** labeled following the nomenclatura of part a. The inset shows a representative surface image at a coverage of ∼1.5 ML. (c) View onto a representative tetramer. (d) Heteromolecular sample of **1** and **3**. **1** marked by circles was first deposited at ∼200 K. Subsequent to a postannealing to RT, complex **3** was deposited at ∼200 K. Complex **3** preferentially forms dimers, see part e. (Scanning parameters: (b) 1 V, 40 pA, 40 × 40 nm^2; (inset) 5.3 V, 80 pA, 400 × 400 nm^2; (c) 1 V, 40 pA, 11 × 11 nm^2; (d) −1 V, 163 pA, 50 × 50 nm^2; (e) 0.5 V, 150 pA, 10 × 10 nm^2.)

which reveal a nearly square like arrangement, only two molecules are aligned to the substrate. The internal arrangement with the *tert*-butyl groups facing the benzene-thiazole side, is suggesting considerable attractive intermolecular interactions and thereby, partially lifting molecule−substrate interaction and avoiding repulsion among adjacent *tert*-butyl groups. Juxtaposed *tert*-butyl groups were not observed as also reported for similar molecular systems[14] as long as molecule-induced substrate restructuring is not thermally driven[15] as in the presented case. The preparation of complexes **1** to **3** at higher coverages of up to two monolayers gave no further indications as long-range ordered structures were not observed and the exact structure of the disordered surface did not allow for a systematic analysis. A representative STM image of a surface after deposition of 1.5 ML of complex **2** is presented in the inset of Figure 3b with areas of the first ML and the second ML indicated. Thereby, molecular layers become insulating and the applied bias voltage had to be respectively increased to larger set values to allow for stable tunneling into unoccupied molecular states at elevated energies.

(14) (a) Yokoyama, T.; Yokoyama, S.; Kamikado, T.; Okuno, Y.; Mashiko, S. *Nature* **2001**, *413*, 619–621. (b) Heim, D.; Seufert, K.; Auwärter, W.; Aurisicchio, C.; Fabbro, C.; Bonifazi, D.; Barth, J. V. *Nano Lett.* **2010**, *10*, 122–128.

(15) (a) Schunack, M.; Petersen, L.; Kühnle, A.; Lægsgaard, E.; Stensgaard, I.; Johannsen, I.; Besenbacher, F. *Phys. Rev. Lett.* **2001**, *86*, 456–459. (b) Rosei, F.; Schunack, M.; Jiang, P.; Gourdon, A.; Lægsgaard, E.; Stensgaard, I.; Joachim, C.; Besenbacher, F. *Science* **2002**, *296*, 328–331. (c) Chen, Y.; Xu, Y.; Deng, K.; Yang, R.; Qiu, X.; Wang, C. *J. Phys. Chem. C* **2009**, *113*, 6725–6729.

Instead, the comparison of the initial growth of complexes **1** and **3** is instructive for the discussion of molecule−molecule interaction. Figure 3d shows a heteromolecular surface after consecutive preparation of complexes **1** and **3** onto the same surface. First, complex **1** was deposited at ∼200 K and its adsorption geometry follows the previously introduced nomenclatura of complex **2**. Different to complex **2** molecular agglomerates were not observed, although sufficient, thermally induced mobility is present during preparation and step edges are completely decorated (see Supporting Information, Figures S1 and S2). This is suggesting that the *tert*-butyl group plays an essential role in the formation of self-assembled structures. Post annealing at room temperature (15 min) did not alter this observation, instead three-dimensional clusters (not shown) at lower frequencies emerged at respectively elevated heights with the internal structure inaccessible. The additional condensation of complex **3** at ∼200 K completes our picture of the molecule−molecule interaction. Different to complexes **1** and **2** dimer formation starts from the initial stage of growth without the need of additional tempering. Even within larger surface areas (see Figure 3d) isolated complexes **3** are barely present among isolated complexes **1**. This reflects an increased interaction strength carried by the additional methyl substitution and is equally observed when only complex **3** is prepared on Cu(111) (see Supporting Information, Figure S3). Two complexes (**3**) of the same chirality are rotated relative to each other by 180° and form dimers with the *tert*-butyl group facing the methyl termination of the opposing complex (see Figure 3e). Nevertheless, already at the given coverage much below 1 ML, irregular structures with two and more complexes involved appear at a considerable level among regular dimers. The exact geometry within these irregular structures could not be satisfactorily resolved, however, with the position of the dominant *tert*-butyl substituent identified, the presence of juxtaposed *tert*-butyl groups can be disregarded as in the case of **2**.

The opposing behavior of interaction for different methyl groups is unexpected. It reveals a more complex insight into intermolecular interactions than previously obtained and indicates aspects of the interaction so far not appropriately considered. Because of the lack of other reasonable alternatives as covalent or ionic bonding as well as van der Waals interaction—the latter is certainly present but is always attractive—it can be assumed that the origin has to be of electrostatic nature. The methyl group is source of a dipolar field—hydrogens are positively charged whereas the carbon is negatively charged, respectively. Depending on the relative alignment, a short-range attraction or repulsion can be expected. The system gets complicated by the presence of the substrate, which will screen the local charge and host image charge underneath the molecule and alter the dipolar field into a multipolar field decreasing rapidly with distance.

Discussion and Summary

Three closely related asymmetric Pd pincer complexes were successfully prepared under vacuum conditions on a Cu(111) surface and their adsorption systematically investigated by STM. The broken symmetry at the surface transfers the structural asymmetry into surface supported chirality. Molecular substituents are identified in STM images by their characteristic appearance in the comparison of all three complexes. Prominent is the role of the methyl groups. Because of an out-of-plane conformation, these methyl groups are the dominant feature in STM images and determine intermolecular interactions. *tert*-Butyl groups energetically prefer binding to methyls (of the methyl−pyridine group), when available, whereas adjacent *tert*-butyl groups repel each other.

Different to the growth of bulk materials from solution, long-range ordered structures are not observed. The observation of highly disordered structures at higher coverages up to 2 ML and after annealing potentially excludes the possibility of studying the growth of regular networks even with other local techniques on the chosen substrate upon further increase of the coverage. However, the observed initial growth of three-dimensional structures for complex **1** after tempering, the tendency to prefer specific molecule−molecule arrangements for complexes **2** and **3**, and the start of insulating behavior beyond 1 ML suggest that further investigations on a less interacting substrate in combination with other local techniques as for example atomic force microscopy might be highly appealing for further development.[16] In the submonolayer range and on an electronically less interacting or partially insulating substrate to lift molecule−substrate hybridization,[17] even scanning tunneling spectroscopy might become a feasible approach to access the electronic states of the isolated complex.

Acknowledgment. S.-H.C., A.S., G.H., and R.W. acknowledge funding through the EU project SpiDME and the Cluster of Excellence NANOSPINTRONICS. C.K. and M.B. wish to thank the DFG for financial support.

Supporting Information Available: Figures S1 and S2 demonstrating that molecular agglomerations of complex **1** are not hindered by the mobility during preparation but step edges are fully decorated and Figure S3 proving that the dimer formation of complex **3** is not modified by the presence of complex **1** but can also be observed when only complex **3** is present. This material is available free of charge via the Internet at http://pubs.acs.org.

(16) (a) Schlettwein, D.; Back, A.; Schilling, B.; Fritz, T.; Armstrong, N. *Chem. Mater.* **1998**, *10*, 601–612. (b) Burke, S. A.; Ji, W.; Mativetsky, J. M.; Topple, J. M.; Fostner, S.; Gao, H. J.; Guo, H.; Grütter, P. *Phys. Rev. Lett.* **2008**, *100*, 186104. (c) Fendrich, M.; Lange, M.; Weiss, C.; Kunstmann, T.; Möller, R. *J. Appl. Phys.* **2009**, *105*, 094311. (d) Topple, J. M.; Burke, S. A.; Fostner, S.; Grütter, P. *Phys. Rev. B* **2009**, *79*, 205414.

(17) (a) Leibsle, F. M.; Flipse, C. F. J.; Robinson, A. W. *Phys. Rev. B* **1993**, *47*, 15865–15868. (b) Qiu, X. H.; Nazin, G. V.; Ho, W. *Phys. Rev. Lett.* **2004**, *92*, 206102. (c) Repp, J.; Meyer, G.; Stojković, S.; Gourdon, A.; Joachim, C. *Phys. Rev. Lett.* **2005**, *94*, 026803.